Robust Nonlinear Controller for Wind Turbine Generator Drivetrain Torsional Oscillation under Large Disturbances

Bi Liu, Junbo Zhao, *Senior Member, IEEE*, Qi Huang, *Senior Member, IEEE*, Federico Milano, *Fellow, IEEE*, Bendong Tan, Weihao Hu, *Senior Member, IEEE*

***Abstract*—This paper proposes a robust nonlinear controller to damp the drivetrain torsional oscillations (DTTOs) of wind turbine generators (WTGs) following large disturbances. The key idea is to integrate a nonlinear sliding-mode control (SMC) with an extended state observer. The former allows transforming the WTG nonlinear model into a simple first-order nonlinear system via the sliding-mode function, whereas the latter can accurately estimate the nonlinear part of the transformed system and effectively compensate the large disturbances. Simulation results show that, under various conditions, the proposed controller achieves significantly enhanced robustness and performance over the linearization-based controller and conventional SMC.**

***Index Terms*—Power system dynamics, wind turbine generator (WTG), drivetrain torsional oscillation (DTTOs), robust nonlinear controller, power system stability control.**

I. INTRODUCTION

With the increased penetration of wind power into electric grid, effective mitigation of drivetrain torsional oscillations (DTTOs) of WTG becomes a technical challenge [1]. Indeed, since the length of drivetrain model is much shorter than that of practical WTG [2], the drivetrain should be modeled by two masses or multiple masses. Hence, the variations of electromagnetic torque or mechanical torque with respect to WTG can result in DTTOs. Moreover, large disturbances, such as shortcircuits [3] and steep variations of wind speed [4] further contribute to give raise to DTTOs, thus significantly reducing the WTG lifespan and increasing its maintenance costs.

Most approaches to deal with WTG DTTOs mainly focus on the compensation of the electromagnetic torque via converters. In [5], a small ripple at the drivetrain frequency is added on the generator torque control and the effect of the resonance is counteracted by the adjusted phase, leading to increased damping of DTTOs. Without a damping controller, the torsional oscillations excited by the grid fault can be very strong. To deal with that, [3] proposes a model-based active damper of the torsional vibration via the linear-quadratic-Gaussian (LQG) algorithm. A STATCOM/BESS-based damping control of DTTOs is developed in [6]. [7] develops a control scheme for active oscillation damping of WTG, where the torque damping controller determines a corrective signal that is added to the reference torque for DTTO control. [4] investigates the drivetrain dynamics under different operating regions of the power-speed curve and develops a DFIG drivetrain stabilizer, where additional damping torque is achieved by a state feedback from the rotor speed to the reference electromagnetic power. In [8], a band-trap filter is proposed to eliminate periodic torque disturbance of the generator torque control loop. This enables the controller to reduce the exciting input of the drivetrain and subsequently damp DTTOs. In [9], [10], a virtual inertial controller is developed for DTTO mitigation, where the first-order derivative of the angular speed about wind generator rotor is used as the input signal to provide an additional electromagnetic torque component of WTG by generator-side converter. In [11], a torsional oscillation damping control based on model predictive control is proposed. With the state feedback control strategy and the model-based torque estimation, the controller compensates shaft torque difference of WTG at the torsional frequency for the active damping of DTTOs. To maximize the energy production of WTG without fatigue damages induced by torsional vibration within the drivetrain subsystem, a receding horizon optimal control framework is proposed [12]. In particular, fault detection and diagnosis as well as controller reconfiguration are integrated to adaptively control the pitch angle.

The aforementioned approaches design DTTO controllers based on first-order Taylor series expansion approximations of the WTG model. This inevitably leads to large errors if large disturbances are considered. To solve this issue, a nonlinear sliding mode control (SMC) has been proposed for the mitigation of DTTOs [13], where the angular speeds of the turbine and generator rotor, along with the drivetrain torsional angle are used as input signals to adjust the rotor current in the generator-side converter of the WTG.

In this paper, we further improve the performance of the SMC by integrating the advantages of SMC and of an extended state observer (ESO) into a unified framework. Specifically, the sliding-mode function is a first-order differential equation that embeds the behavior and control of the nonlinear WTG model. Then the error of this first-order equation is compensated with the proposed ESO, which takes indirectly into account the nonlinearity of the rest of the network. Note that ESO

This research work is supported by The National Key Research and Development Program of China (No. 2017YFB0902002).

B. Liu, Q. Huang and W. Hu are with the Sichuan Provincial Key Lab Science and Technology of China, Chengdu, Sichuan, 611731, PR China. (e-mail: liubi_2006@126.com; hwong@uestc.edu.cn, whu@uestc.edu.cn).

J. Zhao and B. Tan are with the Department of Electrical and Computer Engineering, Mississippi State University, Starkville, MS 39762, USA (junbo@ece.msstate.edu, bt1133@msstate.edu).

F. Milano is with the School of Electrical and Electronic Engineering, University College Dublin, Dublin, Ireland (e-mail: federico.milano@ucd.ie).

also allows estimating the effect of large disturbances, which, thus, do not need to be known *a priori*. The proposed method significantly improves the damping of DTTOs under different system operating conditions as compared to the conventional SMC.

II. Proposed Robust Nonlinear Controller

The ESO is first introduced. Then, the dynamic model and DTTO of WTG are presented and analyzed, followed by the proposed nonlinear controller that integrates ESO and SMC.

A. Outlines of the Extended State Observer

Let us consider the first-order nonlinear system:

$$\dot{x} = f\left(x\right) + g\left(x\right) u \,, \tag{1}$$

where x is the state variable; $f(x)$ is a nonlinear function of x; $g(x) \neq 0$ and u are the control gain function and input, respectively. A second-order ESO for system (1) can be designed as follows:

$$\begin{aligned} \dot{z}_1 &= z_2 - \beta_1 \left(z_1 - x\right) + g\left(x\right) u \,, \\ \dot{z}_2 &= -\beta_2 |z_1 - x|^{\alpha} \mathrm{sign}\left(z_1 - x\right) \,, \end{aligned} \tag{2}$$

where z_1 and z_2 are the state variables of ESO; β_1, β_2 and α are the constant parameters that satisfy $\beta_1 > 0$, $\beta_2 > 0$ and $0 < \alpha < 1$, respectively; sign function equals to 1 for the positive value while to -1 for the negative one.

Under the framework of ESO (2), z_1 and z_2 are designed to approximate x and $f(x)$, respectively. Then, supposing the control objective of state variable x in system (1) to be zero, the control input u can therefore be designed as:

$$u = \frac{-z_2 - K \tanh\left(x/\varepsilon\right)}{g\left(x\right)} \,, \tag{3}$$

where K and ε are the constant parameters; $\tanh(\cdot)$ represents the hyperbolic tangent function. The interested readers can find more details of ESO in [14].

B. Modelling

1) Dynamic model of the wind generator: The following two-mass drivetrain model of WTG [15] is considered in this paper to study DTTOs:

$$\begin{aligned} &2H_{\mathrm{wt}}\dot{\omega}_{\mathrm{wt}} = T_{\mathrm{m}} - K_{\mathrm{sh}}\theta_{\mathrm{sh}} - D_{\mathrm{sh}}\left(\omega_{\mathrm{wt}} - \omega_{\mathrm{g}}\right) \,, \\ &2H_{\mathrm{g}}\dot{\omega}_{\mathrm{g}} = K_{\mathrm{sh}}\theta_{\mathrm{sh}} + D_{\mathrm{sh}}\left(\omega_{\mathrm{wt}} - \omega_{\mathrm{g}}\right) - T_{\mathrm{e}} \,, \\ &\dot{\theta}_{\mathrm{sh}} = \omega_B \left(\omega_{\mathrm{wt}} - \omega_{\mathrm{g}}\right) \,, \end{aligned} \tag{4}$$

where H_{t} and H_{g} are the inertia constants of the wind turbine and generator in seconds, respectively; ω_{t} and ω_{g} denote the angular speeds of wind turbine and generator rotor in rad/s, respectively; ω_B is the nominal angular speed; K_{sh} and D_{sh} represent the stiffness coefficient and the damping coefficient of the shaft, respectively; T_{m}, T_{e} and θ_{sh} are the mechanical power, the electromagnetic torque of WTG and the torsional angle between the rotors of the wind turbine and generator, respectively.

The following modelling assumptions are considered: (a) WTG is modeled with a doubly-fed induction generator (DFIG); (b) all variables are referred to the stator of the generator; (c) the dq reference frame rotates at synchronous angular speed of ω; (d) the positive power directions of stator and rotor are assumed to be out and into the generator, respectively. Thus, the voltage-flux equations of stator and rotor are given by (5) and (6), respectively; (7) and (8) present the corresponding flux-current equations, and the electromagnetic torque is shown in (9).

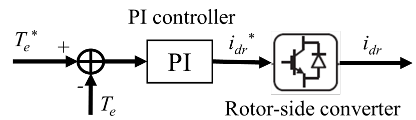

Fig. 1. The control scheme of DFIG active power.

$$\begin{aligned} v_{\mathrm{qs}} &= -R_s i_{\mathrm{qs}} + \dot{\lambda}_{\mathrm{qs}} - \omega \,, \\ v_{\mathrm{ds}} &= -R_s i_{\mathrm{ds}} + \dot{\lambda}_{\mathrm{ds}} + \omega\lambda_{\mathrm{qs}} \,, \end{aligned} \tag{5}$$

$$\begin{aligned} v_{\mathrm{qr}} &= R_{\mathrm{r}} i_{\mathrm{qr}} + \dot{\lambda}_{\mathrm{qr}} + \left(\omega - \omega_{\mathrm{g}}\right)\lambda_{\mathrm{dr}} \,, \\ v_{\mathrm{dr}} &= R_{\mathrm{r}} i_{\mathrm{dr}} + \dot{\lambda}_{\mathrm{dr}} - \left(\omega - \omega_{\mathrm{g}}\right)\lambda_{\mathrm{qr}} \,, \end{aligned} \tag{6}$$

$$\begin{aligned} \lambda_{\mathrm{qs}} &= -L_s i_{\mathrm{qs}} + L_{\mathrm{m}} i_{\mathrm{qr}} \,, \\ \lambda_{\mathrm{ds}} &= -L_s i_{\mathrm{ds}} + L_{\mathrm{m}} i_{\mathrm{dr}} \,, \end{aligned} \tag{7}$$

$$\begin{aligned} \lambda_{\mathrm{qr}} &= L_{\mathrm{r}} i_{\mathrm{qr}} - L_{\mathrm{m}} i_{\mathrm{qs}} \,, \\ \lambda_{\mathrm{dr}} &= L_{\mathrm{r}} i_{\mathrm{dr}} - L_{\mathrm{m}} i_{\mathrm{ds}} \,, \end{aligned} \tag{8}$$

$$T_{\mathrm{e}} = \frac{L_m}{L_s}\left(\lambda_{\mathrm{qs}} i_{\mathrm{dr}} - \lambda_{\mathrm{ds}} i_{\mathrm{qr}}\right) \,, \tag{9}$$

where v, λ, R and i represent the voltage, flux, resistance and current, respectively; the subscript s, r, d, and q denote the stator, rotor, d-axis and q-axis quantities; L_{s} and L_{r} are the stator and rotor, respectively, self inductances; L_{m} is the mutual inductance.

In the dq reference frame with the stator voltage orientation, the d-axis is aligned with the stator voltage vector, yielding $v_{\mathrm{ds}} = U_{\mathrm{s}}$ and $v_{\mathrm{qs}} = 0$, where U_{s} denotes the stator voltage magnitude. By neglecting the transient resistances of stator and rotor, we get

$$T_{\mathrm{e}} = \frac{L_{\mathrm{m}}}{L_{\mathrm{s}}}\lambda_{\mathrm{qs}} i_{\mathrm{dr}} \,. \tag{10}$$

Equation (10) indicates that the active torque T_{e} can be controlled through the rotor d-axis current i_{dr}. The active power control scheme of the DFIG is shown in Fig. 1, where T_{e}^* and i_{dr}^* are the reference values of electromagnetic torque and d-axis current of rotor, respectively.

Neglecting converter switching losses, the power balance of the DC bridge between the back-to-back converters of DFIG is given as:

$$\frac{1}{2C}\frac{d}{dt}v_{\mathrm{dc}}^2 = \frac{1}{C}\dot{v}_{\mathrm{dc}} v_{\mathrm{dc}} = P_i - P_r \,, \tag{11}$$

where v_{dc} and C represent the voltage and capacitance of DC bridge, respectively; P_i and P_r are the active power flowing into the grid-side converter and out from the rotor-side converter, respectively.

2) Model of the DTTOs: The transfer function from the variations of mechanical power ΔT_{m} or electromagnetic torque ΔT_{e} of WTG to the torsional angle variation, $\Delta\theta_{sh}$, can be derived from (4), yielding

$$\Delta\theta_{sh} = \frac{\omega_B(H_g\Delta T_{\mathrm{m}} + H_t\Delta T_{\mathrm{e}})}{2(H_tH_g)s^2 + aH_{tg}s + bH_{tg}}\,, \tag{12}$$

where $H_{tg} = H_t + H_g$; $a = D_{sh}\omega_B$ and $b = K_{sh}\omega_B$. Equation (12) indicates that the variation of mechanical power or electromagnetic torque of WTG may give raise to DTTOs if no damping control is provided. This is because there exists a torsional mode with the natural frequency shown in (13) and the damping coefficient D_{sh} is usually small.

$$\omega_n = \sqrt{\frac{\omega_B K_{sh} H_{tg}}{2H_tH_g}}\,. \tag{13}$$

C. Proposed Nonlinear Controller

To mitigate DTTOs, the torsional angle θ_{sh} and its derivative $\dot{\theta}_{sh}$ are expected to be as close to the equilibrium point of torsional angle θ_{sh0} and zero, respectively, as possible. With this aim, the sliding-mode function candidate consdiered in this work is:

$$\sigma = k\Delta\theta_{sh} + \Delta\dot{\theta}_{sh}\,, \tag{14}$$

where $\Delta\theta_{sh} = \theta_{sh} - \theta_{sh0}$ and k is the coefficient. In turn, the objective of the prposed control is to achieve $\sigma = 0$.

Taking the derivative of the sliding-mode function (14) and combining it with (4), one obtains

$$\dot{\sigma} = f_\sigma + g_\sigma u\,, \tag{15}$$

where the control input u is the compensated electromagnetic torque of the WTG; f_σ is the complex nonlinear function of the states of the WTG and their derivatives introduced in Section II-B; and $g_\sigma = \frac{1}{2H_g}$.

Equation (15) is transformed to fit the ESO framework. Specifically, (15) is in the form of (1). Thus, the ESO in the form of (2) estimates the nonlinear function f_σ and compensate the disturbances, where the state variable x in (2) is σ in (15) and $g(x) = g_\sigma = \frac{1}{2H_g}$.

To effectively suppress the DTTOs, the compensated electromagnetic torque of WTG provided by the proposed controller can be obtained from the control strategy (3), that is:

$$u = 2H_g\left(-z_2 - K\tanh\left(\sigma/\varepsilon\right)\right)\,. \tag{16}$$

Finally, the reference value of WTG electromagnetic torque T_e^* can be derived as:

$$T_e^* = T_{e\mathrm{MPPT}} + 2H_g\left(-z_2 - K\tanh(\sigma/\varepsilon)\right)\,, \tag{17}$$

where $T_{e\mathrm{MPPT}}$ is the reference electromagnetic torque according to the MPPT strategy of WTG [16].

III. Case Study

The performance of the proposed controller following large disturbances is illustrated in this section through simulations. Two scenarios are studied: a power system with a single wind power plant (WPP) and a power system with multiple WPPs. Figure 2 presents the single line diagram of the wind power integrated power system. Each WPP consists of 6 DFIG-based WTGs with 1.5 MW rated power for each DFIG. The parameters for DFIG and the proposed controller are displayed in Table. I.

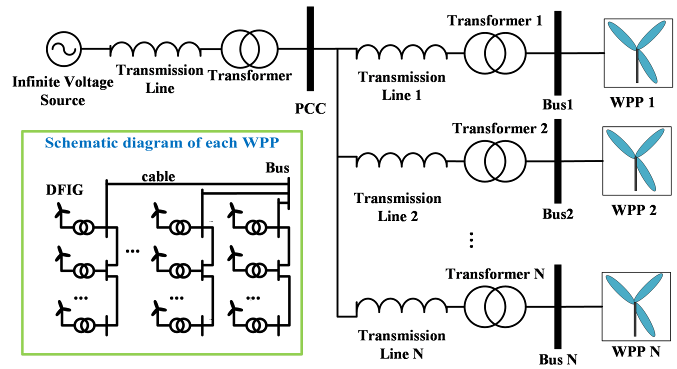

Fig. 2. Schematic diagram of the wind power integrated power system.

TABLE I
PARAMETERS OF THE DFIG AND OF THE PROPOSED CONTROLLER

		DFIG			
H_{g}	0.685 s	H_{t}	4.32 s	D_{sh}	1.5
K_{sh}	1.1 pu/rad	p	3	ω_B	377/3 rad/s
R_{s}	0.023 pu	L_{s}	0.18 pu	L_{m}	2.9 pu
R_{r}	0.016 pu	L_{r}	0.16 pu	ω	377 rad/s
V_{cutin}	4 m/s	V_{rated}	13.4 m/s	V_{cutout}	25 m/s
		Proposed controller			
β_1	10	β_2	10	α	0.5
K	10	k	5		

A linearization-based controller (LC) and a conventional nonlinear SMC [13] are also considered. The compensated electromagnetic toque of the LC is:

$$u = m_1\Delta\omega_{\mathrm{wt}} + m_2\Delta\omega_{\mathrm{g}} + m_3\Delta\theta_{\mathrm{sh}}\,, \tag{18}$$

where $m_1 = 2.2302$, $m_2 = -1.3407$ and $m_3 = -0.0304$, which are obtained according to the linear quadratic optimal theory [17].

The large disturbances considered below are a three-phase shortcircuit occurring at the point of common coupling (PCC) and a steep change of wind speeds. The shortcircuit gives raise to the sudden variation of the WTG electromagnetic power while the latter leads to the instantaneous variation of mechanical power. The derivative of the torsional angle variation $\Delta\dot{\theta}_{sh} = \dot{\theta}_{sh} = \omega_B(\omega_{wt} - \omega_g)$ is proportional to $\omega_{wt} - \omega_g$, and therefore the responses of $\omega_{wt} - \omega_g$ are presented to demonstrate the derivative of torsional angle variation.

A. Power System with a Single WPP

1) Three-phase shortcircuit: A three-phase shortcircuit occurs at $t = 0.5$ s and is cleared at $t = 0.65$ s. The wind speed

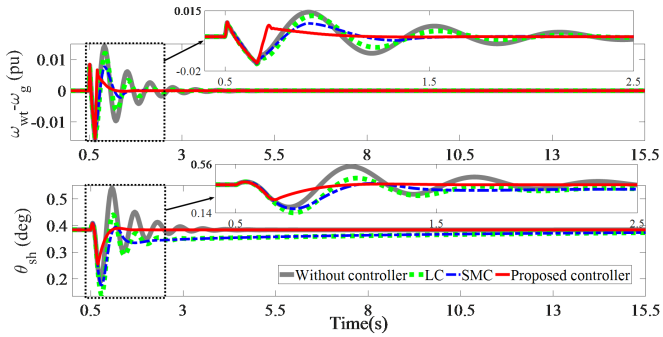

Fig. 3. Dynamic behavior of $\omega_{wt} - \omega_g$ and of the torsional angle with 9 m/s wind speed and following a shortcircuit.

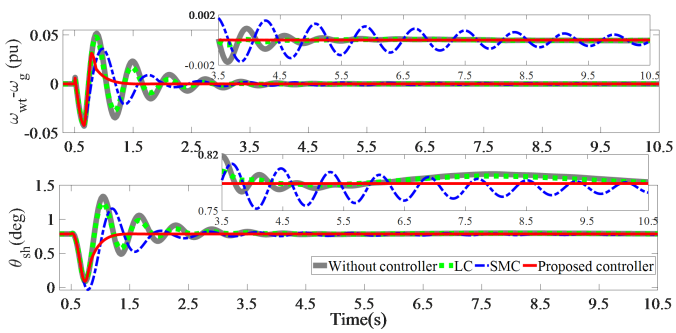

Fig. 4. Dynamic behavior of $\omega_{wt} - \omega_g$ and of the torsional angle with 15 m/s wind speed and following a shortcircuit.

values per each scenarios are 9 m/s and 15 m/s, respectively. The responses of $\omega_{wt} - \omega_g$ and torsional angle are shown in Figs. 3-4. These figures show that the proposed controller achieves the fast speed of damping out the DTTO of WTG and the smallest oscillation magnitude as compared to LC and SMC. Thanks to the capability of handling nonlinearity, the SMC always obtains better performance compared to the LC. It is worth pointing out that the conventional SMC gives raise to the chattering phenomenon for wind speeds under 15 m/s. Chattering is a common shortcoming of the SMC. The proposed controller, on the other hand, can effectively estimate the nonlinear part of the system and simultaneously compensate large disturbances, leading to significantly enhanced performance. Moreover, the proposed controller takes only about 1 s to damp the DTTOs under various wind speeds, while the conventional SMC requires more than 8 s.

2) Steep increment of wind speed: It is assumed that there is a 5 m/s increment to the original 13.5 m/s wind speed at 0.5 s. The comparison results under this scenario are shown in Fig. 5. The SMC has much more improvement in terms of damping DTTO as compared to the previous three-phase short circuit fault. This reason is that this large wind speed changes lead to stronger nonlinearity of the WTG dynamic model and thus the linearization leads to significantly increased approximation errors. As a result, the performance of LC is rather poor. The proposed robust controller further improves its performance and achieves the fastest speed of damping out DTTO.

3) Large stochastic disturbances on wind speed: To further investigate the dynamic performance of the proposed controller and its ability to damp DTTOs following large and

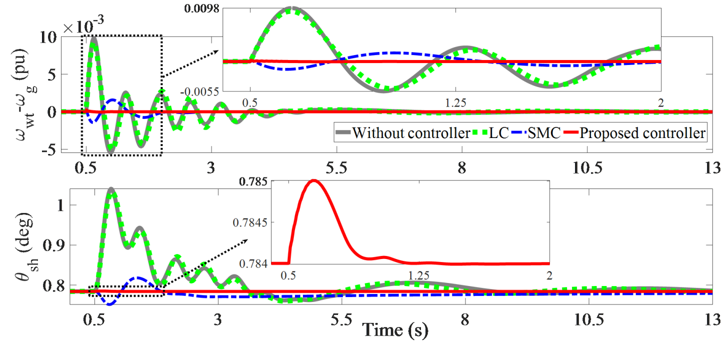

Fig. 5. Dynamic behavior of $\omega_{wt} - \omega_g$ and torsional angles following a steep increment of wind speed.

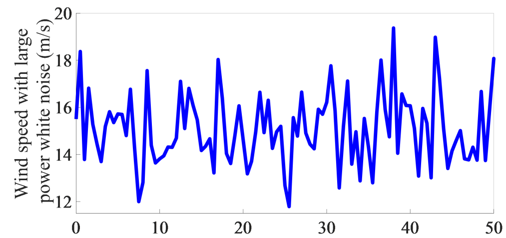

Fig. 6. Sample curve of the wind speed with large stochastic fluctuations.

sudden wind variations, stochastic disturbances are added to the wind speed of the WPP. These stochastic disturbances are simulated with a large white noise. The average wind speed is 15 m/s and the white noise is with 1 power and 1 s sample time. Figure 6 shows a sample curve of the wind speed with large stochastic disturbance. The dynamic behavior of $\omega_{wt} - \omega_g$ and of the torsional angle are depicted in Fig. 7. Results indicate that both LC and SMC are unable to damp the DTTOs and their dynamic response shows large fluctuations. On the other hand, the proposed control strategy counteracts well wind variations and damps efficiently the DTTOs.

B. Power System with Multiple WPPs

In this section, we test the proposed controller through a power system with inclusion of three WPPs, i.e., $N = 3$ in Fig. 2. The parameters of each WPP are the same as those in the previous section. Wind speeds are stochastic and modeled as in Section III-A3. The average wind speeds of WPP1, WPP2 and WPP3 are 8 m/s, 10.5 m/s and 17 m/s, respectively. The corresponding power of the white noise are 0.3, 0.6 and 1.

Figure 8 shows simulation results. Following large stochastic wind speed variations, both the LC and SMC controllers are subject to fluctuations, which are particularly evident for WPP3. This is consistent with the results discussed in the previous section. In general, the SMC yields better dynamic performance than the LC controller. Finally, among the controllers considered in this case study, the proposed method is the fastest to damp the DTTOs and is the least affected by the large fluctuations of the wind.

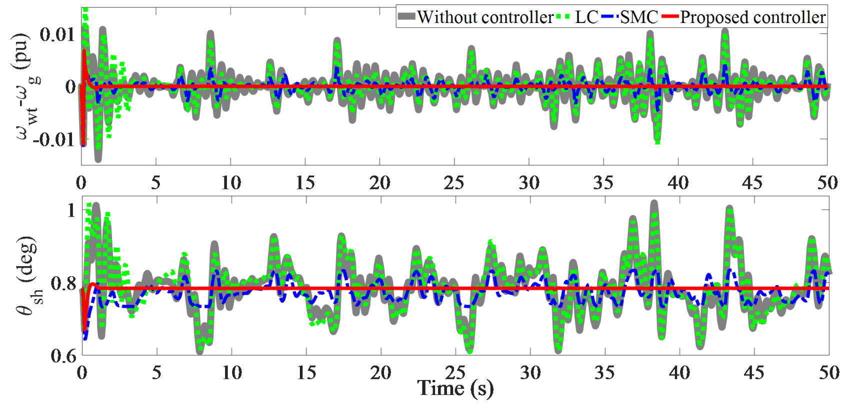

Fig. 7. Dynamic behavior of $\omega_{wt} - \omega_g$ and torsional angle following a large stochastic disturbance on wind speed.

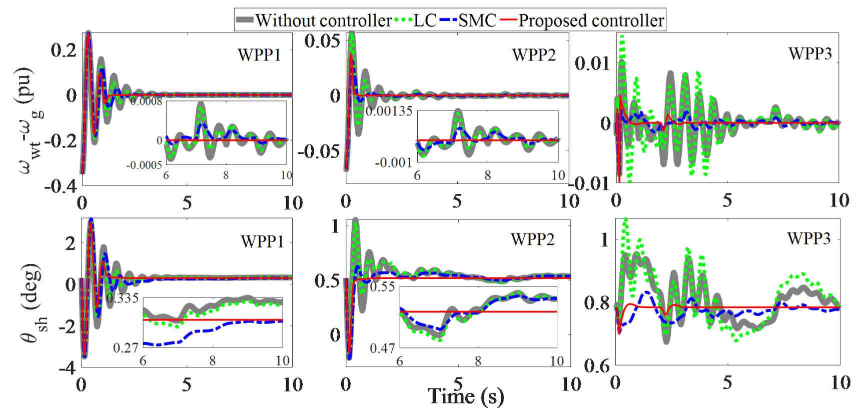

Fig. 8. Dynamic behavior of the torsional angles of WPPs following a large stochastic disturbance on wind speed.

IV. Conclusions

This paper develops a novel robust nonlinear controller to damp DTTOs of WTGs. This control integrates SMC and ESO into an unified approach. Specifically, a first-order nonlinear system is constructed based on the control objectives via the sliding-mode function, and ESO estimates the nonlinear components of the constructed system while compensating the large disturbances. Simulation results show that the proposed controller achieves the best performance under all tested scenarios, including three-phase shortcircuit and large fluctuations of wind speeds. Future works will focus on extending the proposed controller to coordinate WPPs and other distributed energy resources to enhance large-scale power system stability.

References

[1] Y. Zhao, L. Ye, W. Wang, *et al*, "Data-driven correction approach to refine power curve of wind farm under wind curtailment," *IEEE Trans. on Sustain. Energy*, vol. 9, no. 1, pp. 95–105, 2018.

[2] T. Ackerman, "Wind power in power systems," *2nd Edition. Wiley*, 2005.

[3] L. Chen, H. Xu , J. Wenske, "Active damping of torsional vibrations in the drive train of a DFIG wind turbine," *In: Proc. Int. Conf. Renewable Energies and Power Quality, Cordoba, Spain*, 2014.

[4] M. Rahimi, "Improvement of energy conversion efficiency and damping of wind turbine response in grid connected DFIG based wind turbines," *Int. J. Elec. Power.*, vol. 95, pp. 11-25, 2018.

[5] E. Bossanyi, "Wind turbine control for load reduction," *Wind Energy*, vol. 6, no. 3, pp. 229-–244, 2003.

[6] S. M. Muyeen, M. H. Ali, R. Takahashi, T. Murata, "Blade-shaft torsional oscillation minimization of wind turbine generator system by using STATCOM/ESS," *In: Proc. Power Tech. Conf., Lausanne*, 2007.

[7] Z. Xing, L. Liang, H. Guo, X. Wang, "Damping control study of the drive train of DFIG wind turbine," *In: Proc. Int. Conf. Energy and Environment Technology, Guilin, Guangxi*, 2009.

[8] J. Licari, C. E. Ugalde-Loo, J. B. Ekanayake, *et al*, "Damping of torsional vibrations in a variable-speed wind turbine," *IEEE Trans. on Energy Conversion*, vol. 28, no. 1, pp. 172—180, 2013.

[9] I. P. Girsang, J. S. Dhupia, E. Muljadi, *et al*, "Modeling and control to mitigate resonant load in variable-speed wind turbine drive train," *IEEE J. Emerg. Sel. Topics Power Electron.*, vol. 1, no. 4, pp. 277—286, 2013.

[10] G. Mandic, A. Nasiri, E. Muljadi, F. Oyague, "Active torque control for gearbox load reduction in a variable-speed wind turbine," *IEEE Trans. on Industry Appls.*, vol. 48, no. 6, pp. 2424–2432, 2012.

[11] M. Neshati, T. Jersch, J. Wenske, "Model based active damping of drive train torsional oscillations for a full-scale wind turbine nacelle test rig," *in Proc. Amer. Control Conf., Boston, MA, USA*, 2016.

[12] T. Jain, J. Yame, "Fault-tolerant economic model predictive control for wind turbines," *IEEE Trans. on Sustain. Energy*, vol. 10, no. 4, pp. 1696-1704, 2018.

[13] F. Fateh, W. White, D. Gruenbacher, "Torsional vibrations mitigation in the drive train of DFIG-based grid-connected wind turbine," *IEEE Trans. on Ind. Appls.*, vol. 53, no. 6, pp. 5760–57675, 2017.

[14] J. Wang, L. Liu, C. Liu, "Sliding mode variable structure control for seven-dimensional chaotic power system based on extended state observer," *CES Trans. on Elec. Machines and Systems*, 2020.

[15] H. Geng, X. Xi, L. Liu, *et al*, " Hybrid modulated active damping control for DFIG based wind farm participating in frequency response," *IEEE Trans. on Energy Convers*, vol. 32, no. 3, pp. 1220–1230, 2017.

[16] Z. Chen, M. Yin, Y. Zou, K. Meng, Z. Dong, "Maximum wind energy extraction for variable speed wind turbines with slow dynamic behavior," *IEEE Trans. on Power Systems,* vol. 32, no. 4, pp. 3321–3322, 2017.

[17] T. Geerts, "A priori results in linear-quadratic optimal control theory," *IEEE Trans. on Autom. Control*, vol. 8, no. 1, pp. 56–59, 1991.